AAC Accepts, published online ahead of print on 10 March 2014
Antimicrob. Agents Chemother. doi:10.1128/AAC.02739-13

2-aminothiazolones as anti-HIV agents which act as gp120-CD4 Inhibitors

Running Title: 2-aminothiazolones as novel gp120-CD4 Inhibitors

Marika Tiberi,[1] Cristina Tintori,1 Elisa Rita Ceresola,2 Roberta Fazi, [1] Claudio Zamperini,[1] Pierpaolo Calandro,[1] Luigi Franchi,[1] Manikandan Selvaraj,[1] Lorenzo Botta,[1] Michela Sampaolo, [2,3] Diego Saita,[2,3] Roberto Ferrarese,[3] Massimo Clementi, [2,3] Filippo Canducci[3,4,#] and Maurizio Botta[1,5,#]

[1]Dipartimento di Biotecnologie, Chimica e Farmacia, Università degli Studi di Siena, Via A. De Gasperi 2, I-53100 Siena, Italy [2]University Vita-Salute San Raffaele, Milan, Italy [3]Ospedale San Raffale, Milan, Italy [4]Department of Clinical and Experimental Medicine, Università degli Studi dell'Insubria, Varese, Italy [5]Biotechnology College of Science and Technology, Temple University, Biolife Science Building, Suite 333, 1900 N 12th Street, Philadelphia, Pennsylvania 19122.

[*] *To whom correspondence should be addressed. E-mail: botta.maurizio@gmail.com. Phone: (+39)0577-234306. Fax: (+39)0577234333; E-mail: canducci.filippo@hsr.it. Phone: (+39)02-26434284; Fax (+39)0226434288.*

Abstract

We report here the synthesis of 2-aminothiazolones along with their biological properties as novel anti-HIV agents. Such compounds have proven to act through the inhibition of the gp120-CD4 protein-protein interaction which occurs at the very early stage of the HIV-1 entry process. No cytotoxicity was found for these compounds and broad antiviral activity was documented on laboratory strains and pseudotyped viruses. Docking simulations have been also applied to predict the way, at the molecular level, by which the inhibitors were able to interact within the Phe43 cavity of HIV-1 gp120. Furthermore, a preliminary ADME evaluation was performed. Overall, this study led the basis for the development of more potent HIV entry inhibitors.

Introduction

HIV-1 infection continues to be a major health threat worldwide. Approximately 40 million individuals are living with HIV-1 and new infections occur every year. Drug discovery and development have transformed HIV-1 infection into a chronic condition that can be controlled for many years through combination therapies with different classes of antiretroviral drugs, known as highly active antiretroviral therapy (HAART) (1). However, the lifelong duration of HAART and the emergence of resistance to these drugs underscore the need to develop newer inhibitors with reduced toxicity and improved activity and resistance profiles (2-4). The attachment of the human immunodeficiency virus (HIV) to the host cells occurs via binding of the HIV envelope glycoprotein gp120 to the host CD4 receptor, thus, the inhibition of this protein-protein interaction offers an effective way for the development of new antiretroviral agents (5, 6). The crystal structure of gp120 bound to CD4 and the fragment of an antibody (Fab) 17b was solved in 1998(7), revealing that the CD4 binding site of HIV-1 gp120 envelope consists of a hydrophobic pocket, capped by the CD4 Phe43, thus termed the Phe43 cavity. Research into gp120 inhibitors able to block the complex formation between gp120 and CD4 has received increasing attention in recent years and has led to the discovery of active small-molecules characterized by a high degree of chemical diversity. BMS-378806 (BMS-806) and the related compounds #155 and BMS-488043 discovered through a cell-based screening assay, are nanomolar inhibitors that prevent the binding of gp120 to CD4 receptors (8-10). NBD-556 and NBD-557, first discovered by Zhao *et al.* by using an HIV syncytium formation assay on a small library of 33,000 compounds, have been shown to compete with CD4 binding and possess low micromolar potency against several strains of HIV(11, 12). Interestingly, the crystal structure of NBD-556 in complex with gp120 has been recently deposited in the Protein Data Bank (PDB code: 3TGS) highlighting the binding mode of the compound within the Phe43 cavity of gp-120 (13). NBD-556 analogues were then developed to study the structure-activity relationship (SAR) (14-17). Furthermore, molecular modeling techniques were successfully applied

for the identification of new gp120-CD4 inhibitors (18). In this regard, our research group has recently reported the successful application of different virtual screening approaches to the discovery of the hit compounds **1-6** (19, 20). These compounds showed micromolar inhibition of HIV-1 replication in cells infected by wild-type virus, but resulted totally inactive toward the mutant Met475Ile, thus confirming that they target the CD4 binding site on HIV-1 gp120, as residue 475 belongs to the Phe43 cavity. On the other hand, the 2-aminothiazolone derivatives represent a versatile scaffold widely used in medicinal chemistry. Compounds containing the 2-aminothiazolone nucleus have been found to exhibit a broad spectrum of biological activities, such as antitumor (**DBPT**) (21), herbicidal (**7**) and $\alpha_v\beta_3$ receptor antagonist activities (**8**)(22). The 2-aminothiazolone derivatives **9** were recently assayed by us as HIV-1 integrase inhibitors and they resulted to be only moderately active (23).

Herein, novel 2-aminothiazolones were synthesized and biologically tested in order to investigate their potential in inhibiting the HIV infection. Compounds were found able to inhibit the HIV replication at micromolar/submicromolar concentration *in vitro*, resulted to be non-toxic and endowed with a high genetic barrier to the development of resistance at least *in vitro*. Experiments demonstrated that the compounds acted as early inhibitors of the gp120–CD4 interaction. In line with these results, docking studies were next performed to elucidate the binding mode of the 2-aminothiazolones within the Phe43 cavity of gp120 and to identify amino acids involved in their mechanism of action. To the best of our knowledge, this is the first time that 2-aminothiazolone derivatives were investigated as antiretroviral agents targeting the gp120/CD4 interaction.

MATERIALS AND METHODS

Chemistry

General information. All commercially available reagents were used as purchased. Anhydrous reactions were run under a positive pressure of dry N_2. Thin-layer chromatography (TLC) was carried out using Merck TLC plates: silica gel 60 F_{254}. Chromatographic purifications were performed on columns packed with Merck 60 silica gel, 23-400 mesh, for the flash technique. ^{1}H and ^{13}C NMR spectra were recorded at 400 MHz on a Bruker Avance DPX400 spectrometer. Chemical shifts are reported relative to $(CH_3)_4$ Si at δ= 0.00 ppm (Supporting Information). Melting points were measured using a Gallenkamp melting point apparatus and are uncorrected. Elemental analyses were performed on a Perkin Elmer PE 2004 elemental analyzer, and the data for C, H, and N are within 0.4% of theoretical values. T20 (enfuvirtide), AZT (azidothymidine) were obtained from the NIH AIDS reagents repository (https://www.aidsreagent.org/), maraviroc and dolutegravir were obtained from ViiV Healthcare.

The final compounds **16 a-l** were obtained by starting from the commercially available methyl-4-iodosalycilate **10**, which was used in a Suzuki coupling with the 5-formyl-2-furanylboronic acid **11** (Supporting material). The coupled product **12** was then hydrolyzed with an aqueous solution of sodium hydroxide in MeOH/THF to give, after 12 h, the free acid analogue **13**. Next, to generate compounds with general structure **16 a-l**, we adapted a recently published synthethic strategy that describes a one-pot, multicomponent, microwave-assisted reaction that allows the desired final compounds to be obtained directly. The methodology involves 4-(5-formylfuran-2-yl)-2-hydroxybenzoic acid, rhodanine, and primary amines that catalyzed a Knoevenagel condensation between the aldehyde and rhodanine, and then act as nucleophiles in the displacement of the thiocarbonyl sulfur. This method allows to obtain, in very short reaction times and easy workup, several final compounds by changing only the amines employed. We used 4-chloro-3-fluoro

benzylamine, 4-chloro benzylamine, 3,4-dichloro benzylamine, 3-fluoro benzylamine, 4-fluoro benzylamine, 3-chloro-4-fluoro aniline, 4-chloro-3-fluoro aniline, 4-fluorophenethylamine, 4-ethylphenethyl amine, phenethylamine. After dissolving all reagents in EtOH, heating at 150°C for 20 minutes by microwave irradiation was required to effect completion of the reaction. After acidic workup, the wishes products were collected by filtration from ethanol. (Figure 1A) Compound **16m** was obtained through Suzuki reaction from commercial reagents **17** and **11**. Coupled compound **18** reacts with rhodanine and 4-fluorophenethylamine as seen above. (Figure 1B)

HPLC and MS analysis. The purity of the tested compounds was assessed by reversed-phase liquid chromatography and a mass spectrometer (Agilent series 1100 LC/MSD) equipped with a UV detector (λ = 254 nm) and a electrospray ionization (ESI) source. The LC elution method (using a Zorbax Eclipse XDB, 4.6 X 150 mm, 5µm C_8 column) involved the following: (compounds **16a-m)** T = 25° C, mobile phase composed of A) 70% CH_3CN and B) 30% H_2O with 0.5% formic acid at a flow rate of 1.0 mL min^{-1}; (all solvents were HPLC grade, Sigma Aldrich). All analysed compounds meet ≥ 95% purity criteria. MS data were obtained using an Agilent 1100 LC/MSD VL system (G1946C) with a 0.4 mL min^{-1} flow rate using a binary solvent system of 95:5 CH_3OH/H_2O. UV detection was monitored at λ = 254 nm. Mass spectra were acquired in negative mode scanning over the mass range of 50-1500 Da. The following ion source parameters were used: drying gas flow, 9 mL min^{-1} ; nebulizer pressure, 40 psig; drying gas temperature, 350 °C.

Microwave irradiation experiments. Microwave reactions were conducted using a CEM Discover Synthesis Unit (CEM Corp., Mathews, NC, USA). The instrument consists of a continuous focused microwave power delivery system with operator-selectable power output from 0 to 300 W. The temperature of the contents of the vessel was monitored with a calibrated IR temperature control mounted under the reaction vessel. All experiments were performed using a stirring option,

whereby the contents of the vessel are stirred by a rotating magnetic plate located below the floor of the microwave cavity and a Teflon-coated magnetic stir bar in the vessel.

Antiviral activity and cell toxicity

Phenotypic analyses with fully replicating recombinant HIV-1 strains. The human TZM-bl indicator cell line was obtained from American Type Culture Collection (Manassas, VA), and maintained at 37°C in 5% CO2 in DMEM medium containing 10% fetal bovine serum, 50 µg/ml penicillin, and 50 µg/ml streptomycin. HIV-1 viruses NL(AD8) and NL4.3 were titrated as follow: serial fivefold dilutions of each virus were made in quadruplicate wells in 96-well culture plates in a total volume of 100 µl of growth medium for a total of 8 dilution steps. Freshly trypsinized cells (20,000 cells in 100 µl of growth medium containing 75 µg/ml DEAE-dextran) were added to each well and the plates were incubated at 37°C in a humidified 5% CO2-95% air environment. After 48-hour incubation, medium was removed and viral infection was quantified using CPRG assay (Roche). Twenty thousand TZM-bl cells/well were seeded in 96 well plates in complete DMEM supplemented with 30 ug/ml DEAE-dextran (Sigma-Aldrich). 300 TCID50/ml of each strain were pre-treated for 1 hour at 37 °C with six serial dilutions (range 20.000 nM-6.4 nM) of each compound and then added to the cells as described previously (24, 25). Vehicle (0.1% DMSO) treated cells served as negative control. A CCR5 inhibitor (maraviroc) or an integrase inhibitor (dolutegravir) were used as positive control drugs. After 2 days, viral infection was quantified using CPRG assay (Roche). The inhibitory curves were fitted by non-linear regression, allowing IC_{50} calculation by using Prism software. To evaluate cell toxicity of the compounds the metabolic XTT test (Sigma-Aldrich) was performed according to manufacturer's instructions.

Phenotypic analyses with pseudotyped viruses and compounds 16 and 16hl. Pseudoviruses were prepared by transfecting exponentially dividing HEK 293T cells (5 × 106 cells in 15 ml growth medium in a T-75 culture flask) with 5 µg of each env-expression plasmid (from the Tier2 panel: QH0692.42, SC422661.8, TRO.11, AC10.0.29, RHPA4259.7, REJO4541.67, WITO4160.33,

CAAN5342.A2; from the Tier3 panel: PVO.4 and TRJO4551.58) and 10 µg of an env-deficient HIV-1 backbone vector (pSG3ΔEnv) obtained from the AIDS reagents repository, using FuGENE 6 reagent (Roche) as previously described (26, 27). All the envelopes were from subtype B viruses and amplified from R5-tropic viruses during acute infection (28). Pseudovirus-containing culture supernatants were harvested 2 days after transfection, filtered (0.45 µm), and stored at −80°C in 1-ml aliquots. After pseudovirus titration on TZM-bl cells, 40000 TZM-bl cells/well were seeded in 96 well plates in complete DMEM supplemented with 30 µg/ml DEAE-dextran (Sigma-Aldrich). 300 TCID50/ml of each pseudovirus was pre-treated for 1 hour at 37 °C with six serial dilutions (range 20.000 nM-6.4 nM) of compound 16l or 16h and then added to the cells. Vehicle (0.1% DMSO) treated cells served as negative control. A CCR5 inhibitor (maraviroc) was used as positive control drug. After 2 days, viral infection was quantified using CPRG assay (Roche). The inhibitory curves were fitted by non-linear regression, allowing IC_{50} calculation by using Prism software.

Time-of-addition assay

Time-of-addition experiment was performed as previously described with minor modifications (29) by using a single cycle assay and the pseudotype virus REJO4541 clone 67. For the Time-of-addition assay, 40.000 TZM-bl cells/well in a 96 multiwell plate were infected with 1500 TCID50/ml of the env-pseudotyped HIV-1 virus in complete medium supplemented with 30 µg/ml DEAE dextran (Sigma-Aldrich). Virus was incubated with cells for 1 hour at 4° and unbound virus was subsequently removed by extensive and repeated washing with PBS to synchronize the replication (29). To analyse the very early steps of infection we performed a pre-incubation step with the virus and a representative compound (16l) (using IgGb12 obtained from the AIDS reagents repository as comparison) for 1h at 37 °C prior cell infection. For the following four hours, antiretroviral compounds inhibiting distinct viral replication steps (IgGb12, maraviroc, T20, AZT, dolutegravir) and compound 16l were added at the following time points: at time 0, after 60, 75, 90,

120, 150, 180, 210, and 240 minutes. To ensure a completed inhibition of viral replication we used a 40-fold IC_{50} concentration as previously evaluated for each compound on TZM- bl cells (IgGb12 7.5 µg/ml, Maraviroc 0.7 µM, T20 1.6 µM, AZT 3.2 µM, Dolutegravir 1 µM and 16l 5µM). β-galactosidase expression in cell lysates 48h post-infection was used as a marker of HIV infection and was normalized to untreated control cells.

Gp120/CD4-HIS ELISA Binding Assay

Competition between 2-aminothiazolone derivatives and CD4 was performed through a Gp120/CD4-6HisTag ELISA binding assay as previously described with minor modifications (9, 12). Briefly, 96-well multiwell plates (Corning) were coated overnight at room temperature with 100 µL of sheep anti-gp120 antibody D7324 (Aalto Bio Reagents, Dublin) at 5 µg /ml in 100 mM $NaHCO_3$. Wells were blocked with 1% non-fat milk in PBS at 37 °C for 1 h. Coated plate were incubated with 0.5 µg/ml recombinant gp120 (Abcam) in PBS, at 37 °C for 1 h and washed three times with PBS-T 0.1%. Soluble CD4 6His-tagged (Life Technologies) at 0.20 µg/ml in PBS and an equal volume of tested compound at six different concentration (50 µM-1.5 µM) were added to the wells and incubated at 37 °C for 1 h. Vehicle (DMSO) was used as negative control and IgGb12 was used as positive control. Wells were washed five times with PBS-T 0.1% and incubated an hour at 37 °C with a goat anti-His antibody (Roche) at a dilution of 1:1000 in PBS 0.5 % milk. After five wash with PBS-T 0.1%, TMB chromogenic substrate for peroxidase (Pierce) was added and absorbance was read at 450 nm.

Computational studies

Protein Preparation. The HIV-1 gp120 three dimensional coordinates were extracted from the crystallographic complex (PDB entry code 1G9M) (7) and were energy minimized to remove

unfavorable contacts through the all-atom OPLS force field and Polak-Ribiere conjugate gradient method. A continuum solvation method, with water as the solvent, was also applied. Extended cutoffs were used and convergence was set to 0.05 kJ/mol,Å. The homology models of HIV-1 gp120 for NL4.3 (CXCR4-tropic strain) and AD8 (CCR5-tropic strain) were performed with the software PRIME, using two crystallographic complexes (PDB entry code 2B4C (30) and 1G9M) as templates and the primary sequences of the two different strains as queries. The obtained models were energy minimized by the software MacroModel, from the Schrödinger suite, using the Polak-Ribiere conjugate gradient algorithm and OPLS_2005 force field (http://www.schrodinger.com/).

Docking Studies. Compounds were built using the Maestro 9.0 Graphical interface and modeled using the Merk Molecular Force Field (MMFF) in Gibbs Born/Surface Area (GB/SA) water as implemented in MacroModel (http://www.schrodinger.com/). Docking studies were performed using the program GOLD (version 5.1) (31). The ChemScore was chosen as fitness function. The GA parameter settings of Gold were employed using the Search efficiency set to 100%. Finally, results differing less than 1.5 Å in ligand-all atom rmsd (root mean square deviation) were clustered together. For each inhibitor, the first ranked solutions as well as the lowest energy conformation of the most populated cluster were analyzed. Pictures of the modeled ligand/enzyme complexes together with graphic manipulations were rendered with Pymol package (Version 1.2r3pre http://www.pymol.org/).

Molecular Dynamics. Molecular Dynamic (MD) simulations have been performed through the use of AMBER 12 suite of programs (http://ambermd.org/) and the ff03.r1 force field. An appropriate number of counter-ions (7 Cl^- ions for NL4.3 and 3 Cl^- ions for AD8 complex) were added to neutralize the system, and complexes were placed in a octagonal box of TIP3P water molecules. The distance between the box walls and the protein was set to 10 Å. MD runs were carried out with a protocol previously validated (32). Before MD simulation, two stage of energy minimization were performed to remove bad contacts. In first stage, we kept the protein fixed with a constraint of 500 kcal/mol and we minimized the positions of the water molecules. Then, in the second stage, we

minimize the entire system, applying a constraint of 10 kcal/mol on the α carbons. MD trajectories were run using the minimized structure as starting input. Constant volume simulations were performed for 50 ps, during which time temperature was raised from 0 to 300 K using the Langevin dynamics method. Then 150 ps of constant-pressure MD simulations were performed at 300 K in three steps of 50 ps each. During the three periods of this second stage, the α carbons were blocked with harmonic force constants of 10, 5, and 1 kcal/mol·Å, respectively. Finally a 15 ns MD simulation without restraint was run at a constant temperature of 300 K and a constant pressure of 1 atm.

ADME assay

Chemicals. All solvents, reagents, were from Sigma-Aldrich Srl (Milan,Italy). Dodecane was purchased from Fluka (Milan, Italy). Pooled Male Donors 20 mg/mL HLM were from BD Gentest-Biosciences (San Jose, California). Milli-Q quality water (Millipore, Milford, MA, USA) was used. Hydrophobic filter plates (MultiScreen-IP, Clear Plates, 0.45 μm diameter pore size), 96-well microplates, and 96-well UV-transparent microplates were obtained from Millipore (Bedford, MA, USA).

Parallel Artificial Membrane Permeability Assay (PAMPA). Donor solution (0.5 mM) was prepared by diluting 1 mM dimethylsulfoxide (DMSO) compound stock solution using phosphate buffer (pH 7.4, 0.025 M). Filters were coated with 5 μL of a 1% (w/v) dodecane solution of phosphatidylcholine. Donor solution (150 μL) was added to each well of the filter plate. To each well of the acceptor plate were added 300 μL of solution (50% DMSO in phosphate buffer). All compounds were tested in three different plates on different days. The sandwich was incubated for 5 h at room temperature under gentle shaking. After the incubation time, the plates were separated, and samples were taken from both receiver and donor sides and analyzed using LC with UV detection at 280 nm. LC analysis was performed with a Perkin-Elmer (series 200) instrument

equipped with an UV detector (Perkin-Elmer 785A, UV/vis Detector). Chromatographic separation were conducted using a Polaris C18 column (150 - 4.6 mm, 5 µm particle size) at a flow rate of 0.8 mL min^{-1} with a mobile phase composed of 50% ACN/50% H_2O-formic acid 0.1% for all compounds. Permeability (P_{app}) for PAMPA was calculated according to the following equation, obtained from Wohnsland and Faller and Sugano et al. equation with some modifications in order to obtain permeability values in cm s^{-1},

$$P_{app} = \frac{V_D V_A}{(V_D + V_A)At} - \ln(1 - r)$$

where V_A is the volume in the acceptor well, V_D is the volume in the donor well (cm^3), A is the "effective area" of the membrane (cm^2), t is the incubation time (s) and r the ratio between drug concentration in the acceptor and equilibrium concentration of the drug in the total volume (V_D+V_A). Drug concentration is estimated by using the peak area integration. Membrane retentions (%) were calculated according to the following equation:

$$\%MR = \frac{[r - (D + A)]100}{Eq}$$

where r is the ratio between drug concentration in the acceptor and equilibrium concentration, while *D, A,* and *Eq* represent drug concentration in the donor, acceptor and equilibrium solution, respectively.

Water Solubility Assay. Each solid compound (1 mg) was added to 1 mL of water. The samples were shaked in a shaker bath at room temperature for 24-36 h. The suspensions were filtered through a 0.45-µm nylon filter (Acrodisc), and the solubilized compound determined by LC-MS-MS assay. For each compounds the determination was performed in triplicate. For the quantification was used an LC-MS system consisted of a Varian apparatus (Varian Inc) including a vacuum solvent degassing unit, two pumps (212-LC), a Triple Quadrupole MSD (Mod. 320-LC) mass spectrometer with ES interface and Varian MS Workstation System Control Vers. 6.9

software. Chromatographic separation was obtained using a Pursuit C18 column (50 x 2.0 mm) (Varian) with 3 μm particle size and gradient elution: eluent A being ACN and eluent B consisting of an aqueous solution of formic acid (0.1%). The analysis started with 0% of eluent A, which was linearly increased up to 70% in 10 min, then slowly increased up to 98% up to 15 min. The flow rate was 0.3 ml/min and injection volume was 5 μL. The instrument operated in negative mode and parameters were: detector 1850 V, drying gas pressure 25.0 psi, desolvation temperature 300.0 °C, nebulizing gas 45.0 psi, needle 5000 V and shield 600 V. Air and nitrogen were used as nebulizer and drying gas, respectively. Collision induced dissociation was performed using Argon as the collision gas at a pressure of 1.8 mTorr in the collision cell. The transitions as well as the capillary voltage and the collision energy used for compounds **16h** and **16l** are summarized in Table 1. Quantification of the single compound was made by comparison with apposite calibration curves realized with standard solutions in methanol.

Microsomal Stability Assay. Each compound in DMSO solution was incubated at 37 °C for 60 min in 125 mM phosphate buffer (pH 7.4), 5 μL of human liver microsomal protein (0.2 mg mL^{-1}), in the presence of a NADPH-generating system at a final volume of 0.5 mL (compounds' final concentration, 50 μM); DMSO did not exceed 2% (final solution). The reaction was stopped by cooling in ice and adding 1.0 mL of acetonitrile. The reaction mixtures were then centrifuged, and the parent drug and metabolites were subsequently determined by LC-UV-MS. Chromatographic analysis were performed with an Agilent 1100 LC/MSD VL system (G1946C) (Agilent Technologies, Palo Alto, CA) constituted by a vacuum solvent degassing unit, a binary high-pressure gradient pump, an 1100 series UV detector, and an 1100 MSD model VL benchtop mass spectrometer. Chromatographic separation was obtained using a Varian Polaris C18-A column (150 - 4.6 mm, 5 μm particle size) and gradient elution: eluent A being ACN and eluent B consisting of an aqueous solution of formic acid (0.1%). The analysis started with 2% of eluent A, which was

rapidly increased up to 70% in 12 min, then slowly increased up to 98% in 20 min. The flow rate was 0.8 mL min^{-1} and injection volume was 20 µL. The Agilent 1100 series mass spectra detection (MSD) single-quadrupole instrument was equipped with the orthogonal spray API-ES (Agilent Technologies, Palo Alto, CA). Nitrogen was used as nebulizing and drying gas. The pressure of the nebulizing gas, the flow of the drying gas, the capillary voltage, the fragmentor voltage, and the vaporization temperature were set at 40 psi, 9 L min^{-1}, 3000 V, 70 V, and 350°C, respectively. UV detection was monitored at 280 nm. The LC-ESI-MS determination was performed by operating the MSD in the negative ion mode. Spectra were acquired over the scan range m/z 100-1500 using a step size of 0.1 u. The percentage of not metabolized compound was calculated by comparison with reference solutions.

RESULTS

Inhibition of HIV-1 in cell culture

All the synthesized compounds were tested in vitro to evaluate their ability to inhibit HIV replication in human TZM-bl cells infected with HIV-1 NL4.3 (CXCR4-tropic strain) or AD8 (CCR5-tropic strain) and the biological results are listed in Table 2 together with toxicity data. Remarkably, all compounds showed low micromolar/submicromolar activities, with the only exception of compound **16m** that was inactive. Being **16m** the only compound in this series that not contain the salicylic moiety, we can argue that such group is fundamental for the anti-HIV activity of the 2-aminothiazolone derivatives under study. Furthermore, a substituent-dependent effect was observed: the best results were obtained when phenylethylamines were introduced on the thiazolone ring (**16h-l**), while the substitution with shorter chain such as benzylamines (**16a-e**) or phenylamines (**16f-g**) determined a small reduction of the inhibitory potency against HIV-1.

When compounds **16h** and **16l** were tested against Tier2 and Tier3 pseudotyped viruses (all subtype B strains), both compounds showed a similar but not fully overlapping spectrum of neutralization (Table 3). A VSVG control pseudovirus was also used in parallel, but none of the compound showed any inhibitory effect. Reference compound maraviroc showed a 19 ±5 nM IC_{50} with all R5-strains (data not shown). Noteworthy, no toxicity was observed for the tested compounds (LD_{50} > 50μM). Further modifications of the most active compounds **16h-l** are in progress aiming at improving these results.

Mechanism-of-action studies: time of intervention&gp120/CD4 binding assay

A time-of-addition experiment was carried out to exactly determine the target of inhibition of the 2-aminothiazolones. This experiment determines how long the addition of an anti-HIV compound can be postponed within the viral replication cycle before losing its antiviral activity. Reference

compounds with a known mode of action were included. IgGb12 is an anti-gp120 antibody. Maraviroc is a CCR5-receptor antagonist. T20 is a fusion inhibitor that acts by binding to the envelope glycoprotein gp41. The nucleoside analogue AZT inhibits the reverse transcription process while Dolutegravir is an inhibitor of integration process. The same profile of IgGb12 was seen with **16l** (Figure 2). These data confirmed gp120 as a target of interaction of **16l**.

The gp120/CD4 binding assay, demonstrated a direct and dose-dependent inhibition by compounds **16h** and **16l** (IC_{50} =20 μM for both) of the interaction between a dual tropic gp120 that was used in thee assay and soluble CD4 (Figure 3).

Molecular Modeling

Compounds **16a-m** were subjected to docking analysis into a refined gp120 core structure (pdb code 1G9M) [26], by focusing calculations on the Phe43 cavity and its surrounding residues. Analysis of docked complexes suggested that 2-aminothiazolone derivatives made some of the interactions previously identified as crucial for the activity of gp120-CD4 small molecule inhibitors. In detail, the aromatic side chains of the amines at the 2 position were deeply embedded at the bottom of the cavity where established hydrophobic interactions with residues Phe382, Met475, Val255, Trp427, Trp112, Ile424 and Tyr384 while an hydrogen bond was present between the NH and the backbone carbonyl oxygen of Gly473. The thiazolone ring interacts with Ile371, Gly473 and Glu370 by filling the region occupied by the CD4 residue Phe43 in the gp120-CD4 complex. Finally, the salicylic ring was involved in polar contacts with arginine residue at position 476 of gp120 in a solvent-exposed area. As an example, Figure 4A shows the predicted binding mode of compound **16h**. The alignment between the pose predicted for compound **16h** and the binding mode of the NBD-based derivative DMJ-II-121 within the Phe43 cavity (PDB code: 4I54) highlights common interactions between the two inhibitors such as the hydrogen bond with Gly473 and the hydrophobic contacts with Trp112, Phe382, Tyr384 and Ile424. Vice versa, the interaction with Arg476 is exclusively observed for compound **16h** (Figure 4B). Noteworthy, compounds **16f** and

16g were found active against HIV-1 NL4.3 but not on AD8 infected cells. In order to investigate this peculiar behavior, two homology models were built using the primary sequence of both NL4.3 and AD8 strains. A first analysis of the two 3D structures showed no differences into the Phe43 binding site. HIV-1 NL4.3 and AD8 strains differ in their ability to utilize either CCR5 or CXCR4 as coreceptor, and this specificity, is largely determined by the sequence of the V3 loop of the viral envelope protein gp120(33). Accordingly, most of the mutations found in primary sequence are located in the V3 and V4 loops, more than 5Å far from the Phe43 binding site residues into the 3D structures. To evaluate the effects of distal amino acids mutations on the binding profile of **16f**, compound was docked into both the homology models and the two complexes were submitted to 15 ns Molecular Dynamic (MD) simulations. In agreement with biological results, compound **16f** was found more stable in complex with NL4.3 than AD8 and this could explain its different activity profile against the two strains. Figure 5 shows the root mean square deviation calculated on ligand heavy atoms during the time of simulation with respect to the starting pose in complexes AD8 (blue) and NL4.3 (red).

In vitro ADME

We initiated early preclinical in vitro ADME (adsorption, distribution, metabolism, excretion) studies with compounds **16h** and **16l** to determine their aqueous solubility, parallel artificial membrane permeability (PAMPA), and human liver microsomes (HLM) stability in order to early assess the absorption/stability of these drug candidates (Table 2). Passive membrane permeability was evaluated with the PAMPA assay while compound solubility was evaluated following the method developed by Avdeef et al.(34), and results were expressed as LogS (log mol L^{-1}). Metabolic stability was finally evaluated by incubating the above-mentioned compounds with 5 µL of man-pooled HLM for 1 h at 37 °C in order to simulate phase I metabolism. Compounds **16h** and **16l** showed low values of membrane permeation (permeability classification: high >20 x 10^{-6} cm/s,

386 medium 10-20 x 10^{-6} cm/s, low < 10 x 10^{-6} cm/s). However, it has been previously reported that
387 salicylic acid derivatives could pass through cellular membranes by active transport, thus, further
388 experiments in this direction are necessary to better characterize the permeability of these
389 compounds (35). Furthermore, the ADME investigation highlighted good metabolic stability
390 (>99%) and low aqueous solubility (lower than -8 when the desired LogS for a drug candidate
391 should be between -4 and -6).
392
393
394
395

Discussion

Compared to other steps in the replication of HIV-1 that have been successfully inhibited by many available antiretroviral agents, the entry process remains an elusive but extremely interesting target for both therapeutic and preventive approaches against HIV-1 infection (36). Moreover, clinically available entry inhibitors have still several limitations in term of neutralization spectra or pharmacokinetic (PK) properties. In fact, maraviroc (MVC), which targets the interaction of gp120 with the CCR5 coreceptor (37) can only inhibit CCR5-using HIV strains and tropism prediction by genotypic or phenotypic determination is currently mandatory to start MVC treatment (38); enfuvirtide (ENF or T20) that prevents gp41-mediated fusion of the viral and host cell membranes is an injectable peptide associated with still completely unsolved side-effects mainly due to its mode of administration and antigenicity (39, 40). Only two small molecule compounds and their derivatives have recently entered the preclinical and clinical development process (BMS-626529 and NBD-556) and show promising antiretroviral activity (8-12).

In this paper, we showed that a novel class of small molecule compounds can inhibit the earliest CD4-gp120 protein–protein interactions at the host cell viral interface without any cell toxicity in vitro (Table 2). Moreover, we showed that these compounds were able to inhibit CXCR4 and/or CCR5-using laboratory strains and that at least two of these compounds were active against some Tier2 and Tier2 pseudotyped viruses suggesting a wider spectrum of neutralization (27). The tested viruses are very different and have distinct coreceptor usage, however, neutralization assays with more TIER 1 and TIER2 pseudovirus panels, with envelopes coming from non-B subtypes, or antiviral assays on clinical isolates will be needed in order to further extend this observation.

We used the time of addition assay to indirectly demonstrate that the very early entry step is inhibited by these novel molecules and indeed the addition of our representative compound could not be postponed to virus seeding before losing completely its antiviral activity in cell culture. These results were in agreement with the 120/CD4-His competition assay that directly demonstrated

the interaction and inhibition of CD4 binding to gp120. These results suggest that these novel compounds may be used either sequentially or concurrently with currently available HIV-1 entry inhibitors. Although it is theoretically possible that resistance to these novel compounds may also occur through selection of CD4-independent viruses, these variants are rarely selected in vivo and have an increased sensitivity to host immune control compared to CD4-dependent viruses (41) and may thus not be a clinically relevant hurdle to their usage. Thus, the need for novel small molecules with broad neutralization profiles, with reduced toxicity and with favorable PK profiles and are still needed to improve current life-long antiretroviral regimens. In fact, novel combinations of antiretroviral drugs with distinct mechanism of action and with non-overlapping resistance profiles will offer novel strategies to treat or prevent HIV-1 infection.

Next steps for the continuance of drug development of these compounds will be oriented to improve their aqueous solubility. A series of chemical modifications will be performed to introduce polar groups in the part of the molecule exposed to the solvent as well as to increase the binding affinity towards the receptor in agreement with molecular modeling predictions. Furthermore, other strategies to overcome solubility issue could be pursued such as the development of prodrugs or liposome encapsulation (42).

Acknowledgements

This work was supported by the European Union collaborative project "CHAARM" (grant no. HEALTH-F3-2009-242135) and by the Italian Ministero dell'Istruzione, dell'Università e della Ricerca, Prin 2010 research project (grant no. 2010W2KM5L).

REFERENCES

1. Antonelli G, Turriziani O. 2012. Antiviral therapy: old and current issues. International journal of antimicrobial agents 40:95-102.
2. Este JA, Cihlar T. 2010. Current status and challenges of antiretroviral research and therapy. Antiviral research 85:25-33.
3. Asahchop EL, Wainberg MA, Sloan RD, Tremblay CL. 2012. Antiviral drug resistance and the need for development of new HIV-1 reverse transcriptase inhibitors. Antimicrobial agents and chemotherapy 56:5000-5008.
4. De Luca A, Dunn D, Zazzi M, Camacho R, Torti C, Fanti I, Kaiser R, Sonnerborg A, Codoner FM, Van Laethem K, Vandamme AM, Bansi L, Ghisetti V, van de Vijver DA, Asboe D, Prosperi MC, Di Giambenedetto S. 2013. Declining prevalence of HIV-1 drug resistance in antiretroviral treatment-exposed individuals in Western Europe. The Journal of infectious diseases 207:1216-1220.
5. Myszka DG, Sweet RW, Hensley P, Brigham-Burke M, Kwong PD, Hendrickson WA, Wyatt R, Sodroski J, Doyle ML. 2000. Energetics of the HIV gp120-CD4 binding reaction. Proceedings of the National Academy of Sciences of the United States of America 97:9026-9031.
6. Wyatt R, Sodroski J. 1998. The HIV-1 envelope glycoproteins: fusogens, antigens, and immunogens. Science 280:1884-1888.
7. Kwong PD, Wyatt R, Robinson J, Sweet RW, Sodroski J, Hendrickson WA. 1998. Structure of an HIV gp120 envelope glycoprotein in complex with the CD4 receptor and a neutralizing human antibody. Nature 393:648-659.

8. Ho HT, Fan L, Nowicka-Sans B, McAuliffe B, Li CB, Yamanaka G, Zhou N, Fang H, Dicker I, Dalterio R, Gong YF, Wang T, Yin Z, Ueda Y, Matiskella J, Kadow J, Clapham P, Robinson J, Colonno R, Lin PF. 2006. Envelope conformational changes induced by human immunodeficiency virus type 1 attachment inhibitors prevent CD4 binding and downstream entry events. Journal of virology 80:4017-4025.

9. Lin PF, Blair W, Wang T, Spicer T, Guo Q, Zhou N, Gong YF, Wang HG, Rose R, Yamanaka G, Robinson B, Li CB, Fridell R, Deminie C, Demers G, Yang Z, Zadjura L, Meanwell N, Colonno R. 2003. A small molecule HIV-1 inhibitor that targets the HIV-1 envelope and inhibits CD4 receptor binding. Proceedings of the National Academy of Sciences of the United States of America 100:11013-11018.

10. Si Z, Madani N, Cox JM, Chruma JJ, Klein JC, Schon A, Phan N, Wang L, Biorn AC, Cocklin S, Chaiken I, Freire E, Smith AB, 3rd, Sodroski JG. 2004. Small-molecule inhibitors of HIV-1 entry block receptor-induced conformational changes in the viral envelope glycoproteins. Proceedings of the National Academy of Sciences of the United States of America 101:5036-5041.

11. Madani N, Schon A, Princiotto AM, Lalonde JM, Courter JR, Soeta T, Ng D, Wang L, Brower ET, Xiang SH, Kwon YD, Huang CC, Wyatt R, Kwong PD, Freire E, Smith AB, 3rd, Sodroski J. 2008. Small-molecule CD4 mimics interact with a highly conserved pocket on HIV-1 gp120. Structure 16:1689-1701.

12. Zhao Q, Ma L, Jiang S, Lu H, Liu S, He Y, Strick N, Neamati N, Debnath AK. 2005. Identification of N-phenyl-N'-(2,2,6,6-tetramethyl-piperidin-4-yl)-oxalamides as a new class of HIV-1 entry inhibitors that prevent gp120 binding to CD4. Virology 339:213-225.

13. Kwon YD, Finzi A, Wu X, Dogo-Isonagie C, Lee LK, Moore LR, Schmidt SD, Stuckey J, Yang Y, Zhou T, Zhu J, Vicic DA, Debnath AK, Shapiro L, Bewley CA, Mascola JR, Sodroski JG, Kwong PD. 2012. Unliganded HIV-1 gp120 core structures assume the CD4-bound conformation with regulation by quaternary interactions and variable loops. Proceedings of the National Academy of Sciences of the United States of America 109:5663-5668.

14. Curreli F, Choudhury S, Pyatkin I, Zagorodnikov VP, Bulay AK, Altieri A, Kwon YD, Kwong PD, Debnath AK. 2012. Design, synthesis, and antiviral activity of entry inhibitors that target the CD4-binding site of HIV-1. Journal of medicinal chemistry 55:4764-4775.

15. Lalonde JM, Elban MA, Courter JR, Sugawara A, Soeta T, Madani N, Princiotto AM, Kwon YD, Kwong PD, Schon A, Freire E, Sodroski J, Smith AB, 3rd. 2011. Design, synthesis and biological evaluation of small molecule inhibitors of CD4-gp120 binding based on virtual screening. Bioorganic & medicinal chemistry 19:91-101.

16. LaLonde JM, Kwon YD, Jones DM, Sun AW, Courter JR, Soeta T, Kobayashi T, Princiotto AM, Wu X, Schon A, Freire E, Kwong PD, Mascola JR, Sodroski J, Madani N, Smith AB, 3rd. 2012. Structure-based design, synthesis, and characterization of dual hotspot small-molecule HIV-1 entry inhibitors. Journal of medicinal chemistry 55:4382-4396.

17. Lalonde JM, Le-Khac M, Jones DM, Courter JR, Park J, Schon A, Princiotto AM, Wu X, Mascola JR, Freire E, Sodroski J, Madani N, Hendrickson WA, Smith AB, 3rd. 2013. Structure-Based Design and Synthesis of an HIV-1 Entry Inhibitor Exploiting X-Ray and Thermodynamic Characterization. ACS medicinal chemistry letters 4:338-343.

18. Debnath AK. 2013. Rational design of HIV-1 entry inhibitors. Methods Mol Biol 993:185-204.

19. Caporuscio F, Tafi A, Gonzalez E, Manetti F, Este JA, Botta M. 2009. A dynamic target-based pharmacophoric model mapping the CD4 binding site on HIV-1 gp120 to identify new inhibitors of gp120-CD4 protein-protein interactions. Bioorganic & medicinal chemistry letters 19:6087-6091.

20. Tintori C, Selvaraj M, Badia R, Clotet B, Este JA, Botta M. 2013. Computational studies identifying entry inhibitor scaffolds targeting the Phe43 cavity of HIV-1 gp120. ChemMedChem 8:475-483.

21. Teraishi F, Wu S, Zhang L, Guo W, Davis JJ, Dong F, Fang B. 2005. Identification of a novel synthetic thiazolidin compound capable of inducing c-Jun NH2-terminal kinase-dependent apoptosis in human colon cancer cells. Cancer research 65:6380-6387.

22. Dayam R, Aiello F, Deng J, Wu Y, Garofalo A, Chen X, Neamati N. 2006. Discovery of small molecule integrin alphavbeta3 antagonists as novel anticancer agents. Journal of medicinal chemistry 49:4526-4534.

23. Rinaldi M, Tintori C, Franchi L, Vignaroli G, Innitzer A, Massa S, Este JA, Gonzalo E, Christ F, Debyser Z, Botta M. 2011. A versatile and practical synthesis toward the development of novel HIV-1 integrase inhibitors. ChemMedChem 6:343-352.

24. Canducci F, Ceresola ER, Boeri E, Spagnuolo V, Cossarini F, Castagna A, Lazzarin A, Clementi M. 2011. Cross-resistance profile of the novel integrase inhibitor Dolutegravir (S/GSK1349572) using clonal viral variants selected in patients failing raltegravir. The Journal of infectious diseases 204:1811-1815.

25. Canducci F, Marinozzi MC, Sampaolo M, Boeri E, Spagnuolo V, Gianotti N, Castagna A, Paolucci S, Baldanti F, Lazzarin A, Clementi M. 2010. Genotypic/phenotypic patterns of HIV-1 integrase resistance to raltegravir. The Journal of antimicrobial chemotherapy 65:425-433.

26. Burioni R, Mancini N, De Marco D, Clementi N, Perotti M, Nitti G, Sassi M, Canducci F, Shvela K, Bagnarelli P, Mascola JR, Clementi M. 2008. Anti-HIV-1 response elicited in rabbits by anti-idiotype monoclonal antibodies mimicking the CD4-binding site. PloS one 3:e3423.

27. Mascola JR, D'Souza P, Gilbert P, Hahn BH, Haigwood NL, Morris L, Petropoulos CJ, Polonis VR, Sarzotti M, Montefiori DC. 2005. Recommendations for the design and use of standard virus panels to assess neutralizing antibody responses elicited by candidate human immunodeficiency virus type 1 vaccines. Journal of virology 79:10103-10107.

28. Li M, Gao F, Mascola JR, Stamatatos L, Polonis VR, Koutsoukos M, Voss G, Goepfert P, Gilbert P, Greene KM, Bilska M, Kothe DL, Salazar-Gonzalez JF, Wei X, Decker JM, Hahn BH, Montefiori DC. 2005. Human immunodeficiency virus type 1 env clones from acute and early subtype B infections for standardized assessments of vaccine-elicited neutralizing antibodies. Journal of virology 79:10108-10125.

29. Daelemans D, Pauwels R, De Clercq E, Pannecouque C. 2011. A time-of-drug addition approach to target identification of antiviral compounds. Nature protocols 6:925-933.

30. Huang CC, Tang M, Zhang MY, Majeed S, Montabana E, Stanfield RL, Dimitrov DS, Korber B, Sodroski J, Wilson IA, Wyatt R, Kwong PD. 2005. Structure of a V3-containing HIV-1 gp120 core. Science 310:1025-1028.

31. Verdonk ML, Cole JC, Hartshorn MJ, Murray CW, Taylor RD. 2003. Improved protein-ligand docking using GOLD. Proteins 52:609-623.

32. Tintori C, Veljkovic N, Veljkovic V, Botta M. 2010. Computational studies of the interaction between the HIV-1 integrase tetramer and the cofactor LEDGF/p75: insights from molecular dynamics simulations and the informational spectrum method. Proteins 78:3396-3408.

33. Moore JP, Kitchen SG, Pugach P, Zack JA. 2004. The CCR5 and CXCR4 coreceptors--central to understanding the transmission and pathogenesis of human immunodeficiency virus type 1 infection. AIDS research and human retroviruses 20:111-126.

34. Avdeef A. 2001. Physicochemical profiling (solubility, permeability and charge state). Current topics in medicinal chemistry 1:277-351.

35. Koljonen M, Rousu K, Cierny J, Kaukonen AM, Hirvonen J. 2008. Transport evaluation of salicylic acid and structurally related compounds across Caco-2 cell monolayers and artificial PAMPA membranes. European journal of pharmaceutics and biopharmaceutics : official journal of Arbeitsgemeinschaft fur Pharmazeutische Verfahrenstechnik e.V 70:531-538.

36. Sharma AK, George V, Valiathan R, Pilakka-Kanthikeel S, Pallikkuth S. 2013. Inhibitors of HIV-1 entry and integration: recent developments and impact on treatment. Recent patents on inflammation & allergy drug discovery 7:151-161.

37. Klasse PJ. 2013. Structural biology. A new bundle of prospects for blocking HIV-1 entry. Science 341:1347-1348.

38. Nozza S, Canducci F, Galli L, Cozzi-Lepri A, Capobianchi MR, Ceresola ER, Narciso P, Libertone R, Castelli P, Moioli M, D'Arminio Monforte A, Castagna A. 2012. Viral tropism by geno2pheno as a

tool for predicting CD4 decrease in HIV-1-infected naive patients with high CD4 counts. The Journal of antimicrobial chemotherapy 67:1224-1227.

39. Joly V, Fagard C, Grondin C, Descamps D, Yazdanpanah Y, Charpentier C, Colin de Verdiere N, Tabuteau S, Raffi F, Cabie A, Chene G, Yeni P. 2013. Intensification of antiretroviral therapy through addition of enfuvirtide in naive HIV-1-infected patients with severe immunosuppression does not improve immunological response: results of a randomized multicenter trial (ANRS 130 Apollo). Antimicrobial agents and chemotherapy 57:758-765.

40. Huet T, Kerbarh O, Schols D, Clayette P, Gauchet C, Dubreucq G, Vincent L, Bompais H, Mazinghien R, Querolle O, Salvador A, Lemoine J, Lucidi B, Balzarini J, Petitou M. 2010. Long-lasting enfuvirtide carrier pentasaccharide conjugates with potent anti-human immunodeficiency virus type 1 activity. Antimicrobial agents and chemotherapy 54:134-142.

41. Li Z, Zhou N, Sun Y, Ray N, Lataillade M, Hanna GJ, Krystal M. 2013. Activity of the HIV-1 attachment inhibitor BMS-626529, the active component of the prodrug BMS-663068, against CD4-independent viruses and HIV-1 envelopes resistant to other entry inhibitors. Antimicrobial agents and chemotherapy 57:4172-4180.

42. Radi M, Tintori C, Musumeci F, Brullo C, Zamperini C, Dreassi E, Fallacara AL, Vignaroli G, Crespan E, Zanoli S, Laurenzana I, Filippi I, Maga G, Schenone S, Angelucci A, Botta M. 2013. Design, synthesis, and biological evaluation of pyrazolo[3,4-d]pyrimidines active in vivo on the Bcr-Abl T315I mutant. Journal of medicinal chemistry 56:5382-5394.

Compounds	Transition (m/z)	Capillary voltage (V)	Collision Energy (eV)	t_R (min)
16h	214.6	23.5	-100	12.1
	433.2	21.0		
16l	214.6	24.5	-40	12.8
	417.2	20.5		

Table 1. Chromatographic and MS parameters (monitored transition, capillary voltage, collision energy and retention time t_R) of the selected compounds.

606 **Table 2.** Structure, anti-HIV activity and ADME properties of compounds **16a-m**.

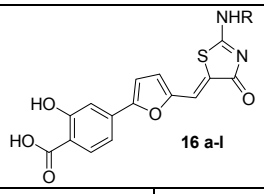

16 a-l

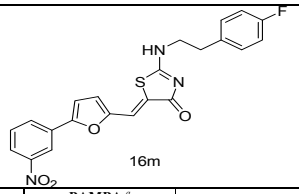

16m

Cpds	R	AD8 IC_{50} (µM)	NL4.3 IC_{50} (µM)	TZM-bl LD_{50} (µM)	PAMPA [a] Papp × 10^{-6} (cm/s) (MR%) [b]	Water Solub. (LogS) [c]	Metab. Stability [d] (%)
16a	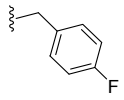	1.0±0.2	1.6±0.5	>50			
16b	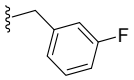	1.3±0.3	3.0±0.4	>50			
16c	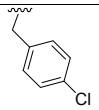	4.3±0.3	3.1±0.5	>50			
16d	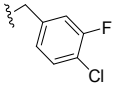	3.0±0.6	2.3±0.4	>50			
16e	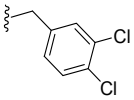	2±0.4	1.8±0.4	>50			
16f	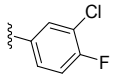	>10	1±0.8	>50			
16g	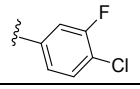	>10	1.8±0.4	>50			
16h	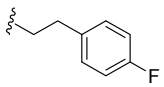	0.6±0.3	0.75±0.3	>50	0.96 (0.0)	-8.8	99.9
16i	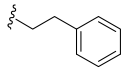	1.5±0.3	0.8±0.1	>50			
16l	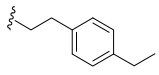	0.85±0.2	1±0.3	>50	0.28 (0.0)	-8.2	99.9
16m	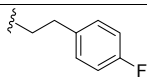	>10	>10	>50			

607
608 [a] PAMPA see experimental section for details; [b] Membrane Retention; [c] LogS= log mol L^{-1}; [d] Expressed as percentage of

609 unmodified parent. Values are expressed as mean +/- SD. Experiments were repeated three times in triplicate.

610
611 **Table 3.** Activity of compounds **16h** and **16l** on laboratory strains (NL4-3 and AD8) and on Tier 2
612 and 3 pseudoviruses. IC_{50}(µM±SD) of Dolutegravir on laboratory strains was 4nM +/-3; IC_{50} of
613 maraviroc on pseudoviruses was 19 ±5 nM IC_{50} . Experiments were repeated three times in
614 triplicate.

Cpds	AD8 IC_{50} (µM)	NL4.3 IC_{50} (µM)	**Pseudo viruses IC_{50} (µM)**									
			QH0692.42	SC422661.8	PVO.4	TRO.11	AC10.0.29	RHPA4259.7	REJO4541.67	TRJO4551.58	WITO4160.33	CAAN5342.A2
16h	0.6±0.3	0.75±0.3	2.9±0.3	1.5±0.2	1.5±0.4	7.7±1.3	1±0.3	>10	1.5±0.4	3.9±0.2	3.9±0.6	5.6±0.3
16l	0.8±0.2	1±0.3	4.1±1.3	4.1±1.3	1.3±0.3	8.7±1.4	1±0.4	>10	1.5±0.5	3.3±0.2	5±0.1	5.6±1.3

615 Values are expressed as mean ± SD.

616

Figure Legend

Figure 1. A) Synthesis of aminothiazolones **16 a-l**: i) Pd(PPh3)2Cl2, Na2CO3, DMF/EtOH, RT, 1h; ii) 1N NaOH, MeOH/THF, reflux, overnight; iii) EtOH, 150 °C, MW, 20 min. **B)** Synthesis of aminothiazolone **16m** *i*) $Pd(PPh_3)_2Cl_2$, Na_2CO_3, DMF/EtOH, RT, 1h; *ii*) EtOH, 150 °C, MW, 20 min.

Figure 2. The time-of-addition assay. The target of the antiviral compound **16l** was identified by comparing its activity in the time scale to that of reference drugs. In the assay a panel of reference drugs sequentially targeting distinct replication steps of HIV-1 from entry to the integration into cell chromosome were used: IgGb12 (an anti-gp120 antibody that binds the CD4-binding site), maraviroc (a CCR5 coreceptor inhibitor), enfuvirtide (T20, a fusion inhibitor), azidothymidine (AZT, an RT inhibitor) and dolutegravir (DTG, as integrase inhibitor). For compound **16l**, efficacy was maximum only when the virus is pre-treated as for IgGb12 and is ineffective once the virus has attached the CD4 cell surface receptor.

Figure 3. Gp120/CD4-His tag binding assay. Two representative 2-aminothiazolone derivatives molecules, 16h and 16l, were tested in a competitive ELISA to demonstrate that gp120 binding to CD4 was the target of this class of compounds. Both compounds were able to displace soluble CD4 from a dual tropic gp120 in a dose-dependent manner (IC_{50} = 20 μM for both compounds). DMSO at the same concentrations present at each compound dilution was also tested. Experiments were repeated twice in triplicate.

Figure 4. A) Binding mode of compound **16h** (blue) as predicted by computational studies. B) Phe43 cavity occupied at the same time by **16h** (blue) and DMJ-II-121 (green, PDB code: 4I54).

Figure. 5. Time evolution of root mean square deviation (RMSD, Å) calculated on heavy atoms of ligand **16f** in AD8 (blue line) and NL43 (red line).